Journal of Solid State Electrochemistry (2018) 22:3597–3606
https://doi.org/10.1007/s10008-018-4074-0

ORIGINAL PAPER

# Measurement of electrochemical noise of a Li/$MnO_2$ primary lithium battery

E. A. Astafev[1] · A. E. Ukshe[1] · Yu. A. Dobrovolsky[1]

Received: 27 March 2018 / Revised: 29 May 2018 / Accepted: 12 August 2018 / Published online: 17 August 2018


## Abstract

Electrochemical noise of a Li/$MnO_2$ primary lithium battery was measured and analyzed during discharge process for the first time. The amplitude of the noise is shown to increase during battery discharge. The power spectral density frequency dependences of the noise are calculated for various stages of the battery discharge. The amplitudes of power spectral densities of the current noise nearly linear depend on the discharge voltage for frequencies below 1 Hz. The slope of the spectral power density frequency dependence of voltage noise changes from − 1 to − 2 during the battery discharge. It was found that the magnitude and slope of the power spectral density frequency dependence of the noise can be considered as a discharge criterion for a primary lithium battery.

**Keywords** Electrochemical noise · Spectral power density · Chemical power sources · Primary lithium battery · Manganese dioxide

## Introduction

A wide application of Li-ion accumulators and primary lithium batteries requires the methods of testing their state of health. Besides, while accumulator can be treated by a full charge-discharge cycle to find out its parameters then it is impossible for a primary battery [1].

At present, besides measurement of discharge characteristics and other voltammetric methods of testing chemical power sources (CPS), the measurement of voltage at constant or impulse load [2–5] is only used. The latter allows obtaining information about immediate state of CPS but can tell nothing about non-stationary destructive processes. These random processes result in a generation of excess electrochemical noise.

At the same time, the method of electrochemical noise is widely used in corrosion studies for a long time [6–8]. It is caused by high amplitude of the electrical noise observed during metal active corrosion that can be easily measured. In other electrochemical studies as well as in the investigation of CPS, the noise measurement is a complicated engineering task. Nevertheless, the method of electrochemical noise measurement is known from the middle of the previous century. V.A. Tygai is one of the pioneers in this area [9–11]. His works were fundamental ones involving a precise experiment and deep theoretical understanding. Owing to all these reasons, V.A. Tyagai created a basis of the method. At the same time, G.C. Barker [12–14] carried out studies of not particular practical interest. B.M. Grafov's original studies [15–17] as well as the contemporary ones [18–20] made a great impact on the analysis and theoretical interpretation of electrochemical noise.

The analysis of electrochemical noise is a complicated task; there is no general procedure for it. The only evident observation is the fact that measured noise signal can provide much more information than the value of its average amplitude or power. The data presented in the literature covers the subject systematically in a number of reviews [8, 21]. Obviously, the method of the analysis of power spectral densities (PSD) of electrochemical noise gives certain information about physical processes and phenomena [6, 7, 22–25]. We have also utilized this analysis in the study of fuel cell electrochemical noise [26].

In the present study, we examined electrochemical noise of primary lithium batteries GP CR2032 (GP Batteries International Limited). These samples are widely available

✉ E. A. Astafev
tdsipch@list.ru

[1] Institute of Problems of Chemical Physics RAS, acad. Semenov av., 1, Chernogolovka, Moscow region, Russia 142432

and their form factor is suitable for investigation. The anode of the element is Li and the cathode is $MnO_2$ [26]. The electrochemical response of such elements is well studied [27–36], but there is no study of the electrochemical noise of mass-produced primary lithium batteries. According to the manufacturer, main parameters of the investigated battery are as follows. Nominal voltage is 3 V, nominal capacity is 220 mAh, continuous discharge current is 3 mA, and maximal impulse discharge current is 20 mA.

Thus, the goals of the present study are as follows: the measurement of electrochemical noise of $Li/MnO_2$ primary batteries and the establishment of main regularities of changes in noise behavior during the discharge on a resistive load.

## Experimental

Electrochemical noise was measured during discharge of the tested battery loaded with a constant value resistor. Several resistor setups with values of 800, 2040, and 4800 Ohm were used. Long-discharge regimes with resistors of high values are the most interesting ones that correspond to the real operation [27] of the batteries under consideration. However, it causes the experiment to be very prolonged. Several batteries from one series (technological pack) were utilized in the measurements. Each battery was discharged only once and recycled afterwards. Electrochemical noise was measured by means of a specialized device electrochemical instruments NM-4 [37]. It was constructed on the basis of a high-resolution analog-to-digital converter (ADC) and a low-noise preamplifier with high-input impedance. We used analog devices AD7177-2BRUZ 32bit high-precision ADC with 3 Linear Technology LTC6655BHMS8–2.5 0.25 ppm references placed in parallel to achieve a very wide dynamic range. The references were used according to datasheet. At the output of each of them, ballast precision 33-Ohm resistor was placed. The outputs of all three resistors were connected together to form the ADC's reference source. This procedure reduces the total reference noise level to square root from number of paralleling reference chips (it is 1.73 times in our case).

The ADC was used with all the manufacturer's recommendations according to the datasheet. Sample rate was up to 500 points per second. The gain of the amplifier was 100. For such a configuration, the inherent noise of the instrument was less than 1500 $nV/Hz^{0.5}$ that is equivalent to a thermal noise of 1500-Ohm resistor in the frequency band of 250 Hz. For the gain chosen in preamplifier, the range of measured voltage was from − 24 to 24 mV with a quantization of less than 1 nV. The instrument has two identical channels with individual configurations. For the measurement of electrochemical noise in described regime, only one channel was used. To eliminate the DC current component, the input was equipped with a first order RC-filter (cutoff frequency is of 0.01 Hz) based on low-noise precision resistor and capacitor. This input filter was made of 16 ceramic capacitors Murata GRM32ER60J107ME20L 100 μF 6.3 V assembled in parallel by means of suspended mount to prevent piezoelectric effect. The filter resistor was Yageo thin film 0.1% 15 ppm precision resistor 1/6 W, 10 K MFP-12BTC52. The second channel operated with a 0.5 gain of measured DC voltage to obtain the discharge curve synchronized with the noise measurement. A real range of the input voltage of the second channel was from − 5 to 5 V. The measurement setup was thoroughly doubly shielded with the use of the cage with 1-mm steel walls. Inside a cage, there was an aluminum box with 2-mm walls as a container for instruments board and object under test.

The electrochemical noise measurements were carried out in two steps. There were serial measurements with different sampling rates, namely 500 and 20 points per second. Every data array consisted of 30,000 samples for each measurement. Collecting all data as a single array on one high-sample rate would require 25 times larger data array which would raise a lot of problems with data storage as whole data points are stored in a flash-memory of the instrument (it is necessary for data safety during several days measurement). Additionally, manipulating two single-data arrays is much comfortably then a large single one. Also, connection of two spectrums in high- and low-frequency bands in frequency domain can show experimental problems (non-stationary effects for example) if they would exist. If there would be no problem, the spectrums would look like one. In another case, they would not connect together.

After that, a pause has been held (depending on the load value, from 1 h for 800 Ohm to 6 h for 4800 Ohm). Then the whole cycle is repeated several times, each one at the curtain voltage of discharging curve, until the battery discharge voltage becomes lower than 2 V. A load resistor was connected to the battery during all the experiment time. The measurement was fully automated and did not involve operator's contact with the object under test to minimize interference and industrial-frequency picking up.

The inherent noise of the NM-4 instrument was measured after every turn-on and warming-up. These measurements were carried out at the same sample rates and data arrays were of the same size as for investigated objects. Initial processing of the instrument inherent noise that is "detrending" and calculation of PSDs was carried out in the same way as for investigated battery. After that, the frequency dependence of PSD of the measurement instrument inherent noise was subtracted from the PSD of the object noise. Additionally, the instrument was tested with high-precision constant resistors, for which the thermal noise was measured and corresponding resistance values were calculated according to the Nyquist equation [38]:

$$R = S_V/4k_bT, \quad (1)$$

where $S_V$ is a PSD of the voltage noise, $k_b$ is a Boltzmann constant, $T$ is an absolute temperature, $R$ is an equivalent noise resistance. Inherent noise of the instrument was also subtracted from the measured signal for this calibration procedure. As a result, horizontal frequency dependencies of equivalent noise resistance were obtained from which the value of the resistor under test was evaluated. It agreed with the manufacturer resistor value within the 5–7% accuracy.

Figure 1 represents some examples of electrochemical noise of investigated batteries obtained at several voltages of discharging curve. The figure denotes data portions recorded during a 25-s time period obtained at 20 points per second sampling rate and detrended with a first-order polynomial. The curves are shifted in the vertical direction to improve the visual representation. Inherent noise of the instrument is also shown on the figure. As it can be seen, the amplitude of the noise increases as the battery becomes more discharged and its voltage becomes lower.

Electrochemical instruments (Russia) P-40X potentiostat-galvanostat with the FRA-24M frequency response analyzer module was used in electrochemical impedance measurements. The amplitude of AC signal was 5 mV. Frequency range was from 50 kHz to 27 mHz. The measurements were carried out in the following way. In a galvanostatic regime, the battery was discharged by DC current of 2 mA (that is the closest to the regime of discharging by a constant resistor of 1200–2400 Ohm). Then in a potentistatic regime, the impedance was measured at the potential achieved during discharging in a galvanostatic regime. Prior to the frequency scan, a battery was polarized at DC voltage during 4.7 h to approach a quasi-steady state condition at the same constant potential. The whole procedure was repeated automatically by the programmer 20–30 times until the battery discharge voltage became lower than 2.2 V. All of the impedance measurement stages were carried out without a load resistor. The impedance hodographs are presented as the Cole-Cole diagram in Fig. 2 with the corresponding points on the discharging curve.

## Data processing and analysis of results

The simplest way to analyze the noise amplitude is the evaluation of standard deviation (SD) of voltage from the mean value on the output of the battery [8, 21]. It can be used for chemical power sources electrochemical noise investigation and analysis [39]. Figure 3 shows the dependence of standard deviation on the value of constant voltage of the discharging curve. As it can be seen, there is a near linear increase in the decimal logarithm of noise amplitude as the battery becomes more discharged. These data were obtained as a result of detrending with the moving average by 100 points. The data array of 30,000 points obtained at 500 samples per second was processed. The discharge procedure was carried out with the load resistors value of 2040 Ohm. In fact, due to the detrending procedure that is a 1st-order high-frequency

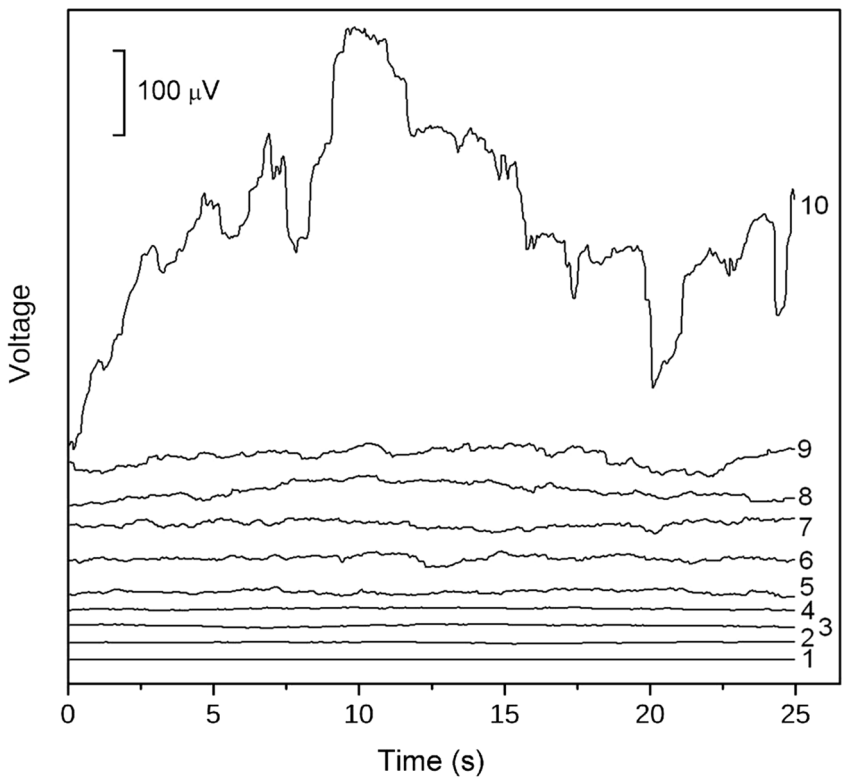


**Fig. 1** A general view of electrochemical noise during battery discharge on the constant resistor of 2040 Ohm at different voltages of discharging curve, V:1—the noise of the device, 2—2.894, 3—2.882, 4—2.875, 5—2.752, 6—2.682, 7—2.607, 8—2.542, 9—2.434, 10—2.126

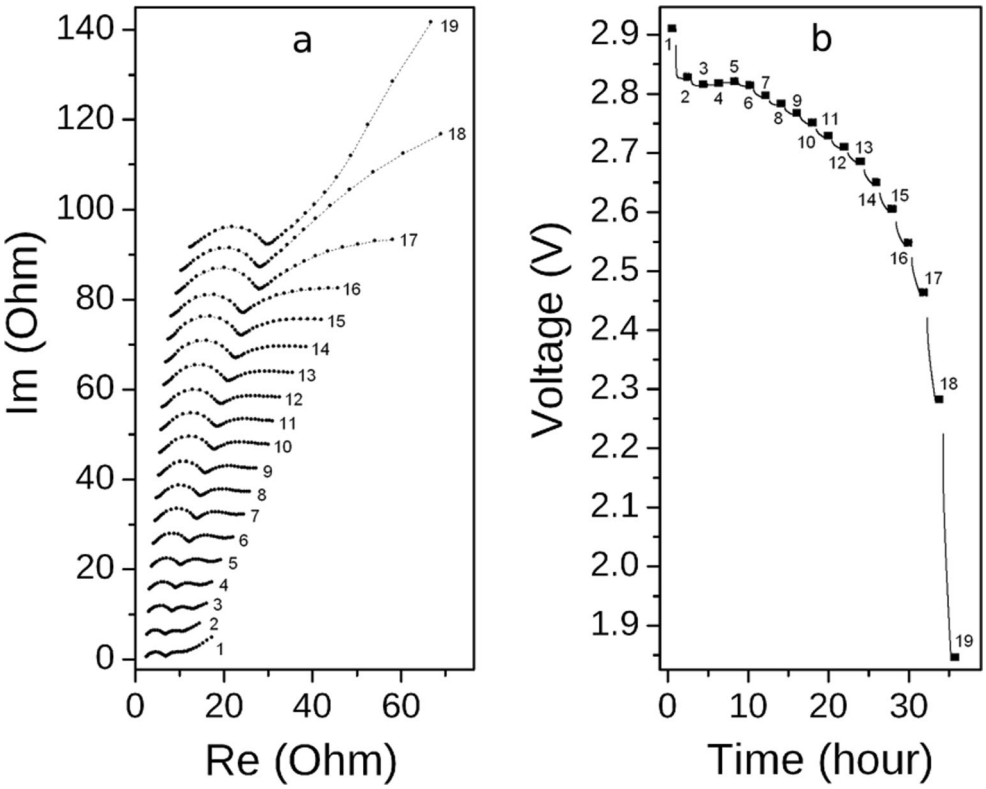


**Fig. 2** **a** Hodographs of impedance for different voltages of the discharging curve. Hodographs are shifted along the vertical ax for 5 Ohm. **b** Corresponding discharging curve that includes the stages of discharge and impedance measurement except the stage of DC polarization at constant potential before impedance measurement (4.7 h each)

filter with cutoff frequency close to $f_A/100 = 5$ Hz ($f_A$ is a sample rate of ADC), the figure corresponds to the behavior of the system under investigation at frequencies higher than 5 Hz. The level of the instruments noise measured and processed in the same way is $7.78 \cdot 10^{-8}$ V that is close to the value of 5 nV/Hz$^{0.5}$ in the frequency band of 250 Hz. However, the method of evaluation of standard deviation gives no information except the mean value of noise amplitude.

Calculation of PSD was carried out with the division of each analyzed data array of 30,000 points into 60 segments of 500 points. Each of the segments was individually detrended by linear approximation. Obtained spectral power densities were averaged [40, 41]. Detrending procedure corresponds to a first-order filtration with cutoff frequency of 1 Hz for 500 points per second sample rate and 0.04 Hz for 20 points per second. We successfully used this method of trend removal and PSD calculation in our previous works

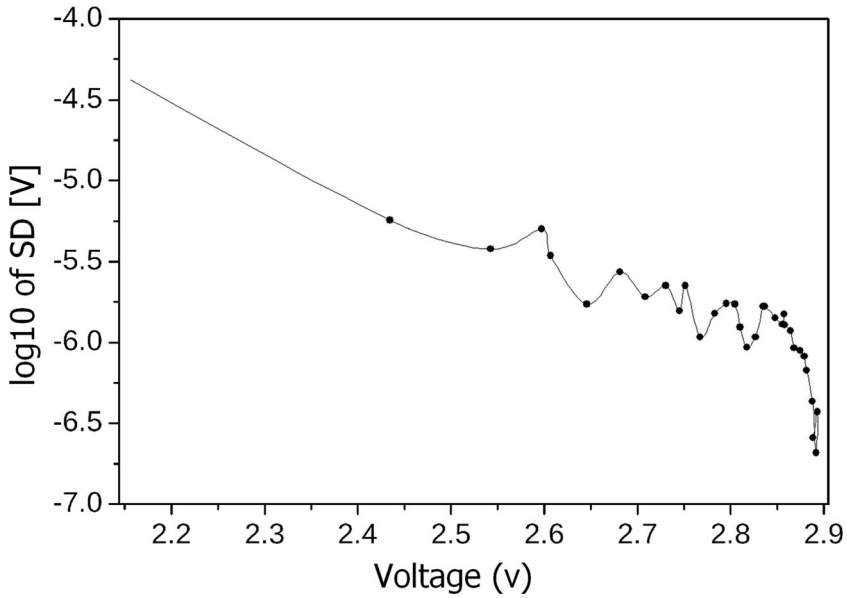


**Fig. 3** A dependence of standard deviation of voltage at the load on the voltage in the discharging curve at discharge on the 2040-Ohm resistor

[42–44]. We also tried a lot of other types of detrending procedures and found this one to be the most appropriate. The results for two load resistors are presented in the Fig. 4.

As it can be seen from Fig. 4, frequency dependencies of the voltage noise PSDs are almost linear lines with a constant slope in the double-logarithmic coordinates. At frequencies higher than 10–100 Hz there is a little distortion due to the finite noise of the measurement instrumentation. Despite the fact that inherent noise of the hardware is subtracted on this stage, the accuracy of this subtraction is finite and results in a distortion of the lines as electrochemical noise in such conditions appears to be much lower than the noise of the hardware. There is also a little distortion at low frequency that looks like an approach to the low-frequency plateau. This effect is caused by influence of the input filter of the device which cuts off a DC voltage component.

Every frequency dependence of the PSD is obtained from two separate data arrays recorded at one discharge curve potential. The low-frequency one is obtained at the sampling rate of 20 points per second and the high-frequency one at 500 points per second. As it can be seen from Fig. 4, the joints of two spectrums are almost impossible to observe and they form one continuous spectrum. This indicates that the measurement is made in near steady-state conditions, since the chosen detrending procedure did not distort the spectrums at the edges. Otherwise, the overall trend of the discharge voltage would not be linear in the single high- or low-frequency spectrum under consideration, and detrending with the first-order polynomial would not succeed, namely there would be an overstatement of the power spectral density values especially at the edges of the frequency range.

The growth in the PSD values is observed during battery discharge for both load resistors. There is an increase in the slope of frequency dependencies, in double-logarithmic coordinates. According to the phenomenological approach of the Flicker-noise approximation [45, 46], an exponent $n$ or the slope of the spectrum linear approximation in logarithmic coordinates is the parameter which provides information. On the other hand, such dependence can be caused by the filtration of generated noise by double-layer capacity of the electrodes. All spectral power densities were approximated by straight lines to analyze $S \sim f^n$ dependences. At the same time, frequency regions of instrumental distortions were not taken into consideration. The results for all three-load nominals are shown in Fig. 5.

The slopes of the PSD frequency dependences for different battery discharge stages are close for all three load resistor values at the same voltages on discharge curves. The nature of these dependences changes in a similar way in the 2.7–2.9 V discharge voltage region.

There is a rapid increase in the slope from $n = -1$ to $n \sim -1.8$ in the region of a small discharge degrees at a battery voltage of 2.7–2.9 V. There is also an inflection in the region of these voltages on the discharge curve. In practice, we guess that the value of 2.6 V can be considered a criterion of the discharged battery. The value of the PSD slope of electrochemical noise can probably be considered as a criterion of possibility of further operation and usability of batteries of this type when the noise is measured during battery discharge on a constant load.

The dependencies of PSD values on the discharge curve voltage were plotted for several frequencies (Fig. 7) to investigate the increase in current noise PSD values during the discharge process.

It is possible to say that there is nearly a linear dependence of the current noise PSD values on the voltage of the discharge

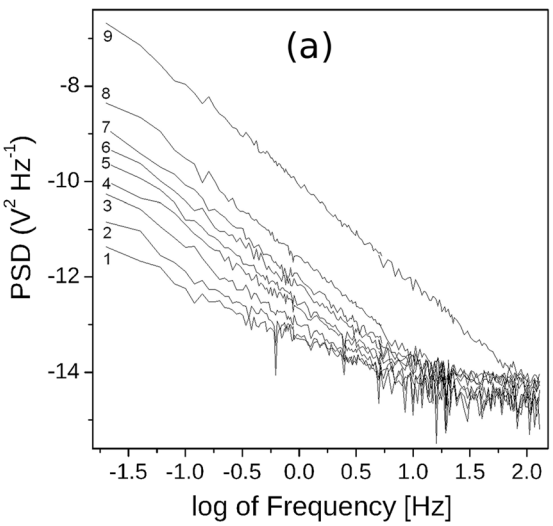


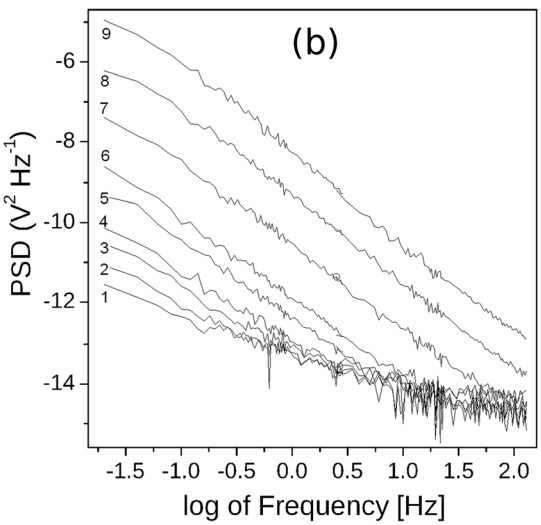


**Fig. 4** A logarithm of voltage noise spectral power density in the course of the discharge for different voltages of discharging curve. **a** 2040-Ohm load resistor: 1—2.894 V, 2—2.882 V, 3—2.875 V, 4—2.752 V, 5—2.682 V, 6—2.607 V, 7—2.542 V, 8—2.434 V, 9—2.126 V. **b** 4800-Ohm load resistor: 1—2.939 V, 2—2.935 V, 3—2.929 V, 4—2.784 V, 5—2.708 V, 6—2.660 V, 7—2.554 V, 8—2.385 V, 9—1.962 V

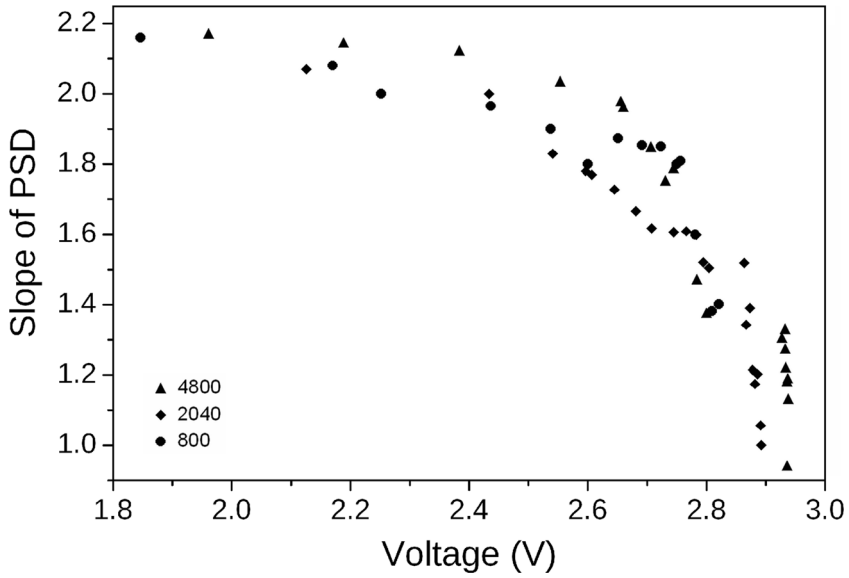


**Fig. 5** Dependencies of the slopes of PSDs of voltage noise on the position of measurement point (battery voltage) on the discharging curve for different load resistors (the values of load resistors are indicated in the figure legend). The values of slopes are multiplied by −1

curve up to discharge voltages of about 2.5 V at low frequencies (curves 5 and 6 in Fig. 7), that is at voltages of a battery which is valid for operation. At higher frequencies, more complex dependencies are observed. The nature of the dependences for all frequencies changes at voltages of a deeper discharge. That is, at a deep discharge, not only the PSD spectrum but also the noise amplitude weakly depends on the degree of discharge and approaches its maximum.

For comparison of impedance spectra and noise PSD spectra, we used the modification of simple equivalent circuit of electrodes of buttery under investigation. Figure 8 shows a basic part of the equivalent circuit which explains the proposed electrochemical noise behavior model of the investigated electrochemical system [10, 12]. In this circuit, the constant phase element $C$ can be associated with the Warburg element or with the double-layer capacitance. Resistance $R$ can be attributed to the Faradic resistance, the resistance of the SEI film or the shunting resistance of the Warburg element. Such circuit is a part of commonly used equivalent circuits. They are used in electrochemical impedance data analysis [47–49]. The frequency-independent noise source $U$ can be introduced either in series with the resistance or in parallel with it as a source of current noise according to the equivalent noise generator theorem [50]. At medium and high frequencies for such a scheme, there would be a linear frequency dependence of the power spectral density of the noise with a slope corresponding to the doubled exponent of the considered constant phase element C. We successfully used such and more complex model to quantitatively describe the behavior of electrochemical noise of a fuel cell under different loads [42, 43]. In the case, where this scheme is externally shunted by the other RC circuit which consists of another impedance elements of electrochemical cell, the total slope observed on SPD frequency dependences can

**Table 1** The values of frequency-dependence slopes of voltage noise PSDs and the values of frequency-dependence slopes calculated from the main components of the impedance equivalent circuit. The values of slopes are multiplied by − 1

| Voltage, $V$ | PSD slope ($f$) | Slope from the low-frequency semicircle | Slope from the CPE of high-frequency semicircle | log (Re ($f$)) slope |
|---|---|---|---|---|
| 2.9 | 0.94 | – | 1.40 | 0.17 |
| 2.89 | 1.18 | – | 1.38 | 0.13 |
| 2.87 | 1.36 | – | 1.45 | 0.12 |
| 2.85 | 1.45 | – | 1.52 | 0.10 |
| 2.84 | 1.50 | – | 1.56 | 0.074 |
| 2.75 | 1.70 | 0.44 | 1.64 | 0.083 |
| 2.69 | 1.80 | 0.72 | 1.65 | 0.10 |
| 2.588 | 1.90 | 0.81 | 1.63 | 0.15 |
| 2.46 | 2.01 | 1.14 | 1.60 | 0.30 |
| 2.31 | 2.06 | 1.54 | 1.58 | 0.44 |

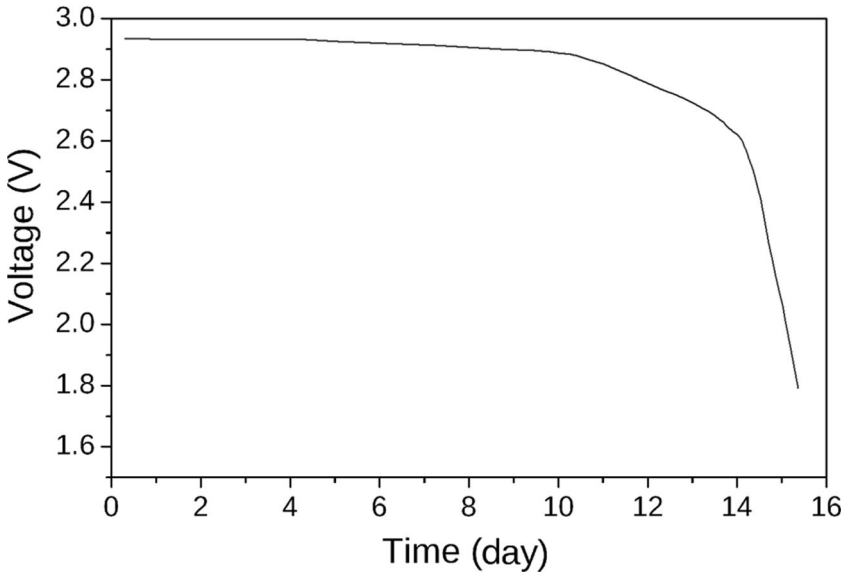


**Fig. 6** Discharge curve at a load of 4080 Ohm

increase and exceed the value of −2 which we observe in our measurements and in other works focused on similar systems [24].

The values of these elements of equivalent circuit were calculated with the use of the data obtained from the electrochemical impedance method for a deeper analysis. It should be noted that electrochemical noise behavior modeling is out of aims of current work and supposed to be done in future works, but some comparisons of two methods results can be made. Table 1 shows the values of doubled exponents of two constant phase elements for low-frequency and high-frequency semicircles, which are clearly distinguishable on the impedance spectra (Fig. 2). It is well known that for an ideal capacitor such a value is equal to −2, for the Warburg element it is equal to −1. As it can be seen, the high-frequency semicircle changes the angle of the corresponding constant phase element, and its dependence on the voltage and the degree of battery discharge weakly correlates with the dependence for PSD slope. The low-frequency constant phase element, which although does not agree numerically with the PSD slope, has the same tendency of systematic growth as for PSD below some discharge voltage. There are no values of the indicators for discharge voltages higher than 2.8 V in the table, because the semicircle transforms into a practically horizontal section and cannot be precisely analyzed in the corresponding frequency region. The table also shows the dependence of the active component of the impedance on the degree of discharge. As it can be seen from the analysis of these values, the measured noise does not correlate with

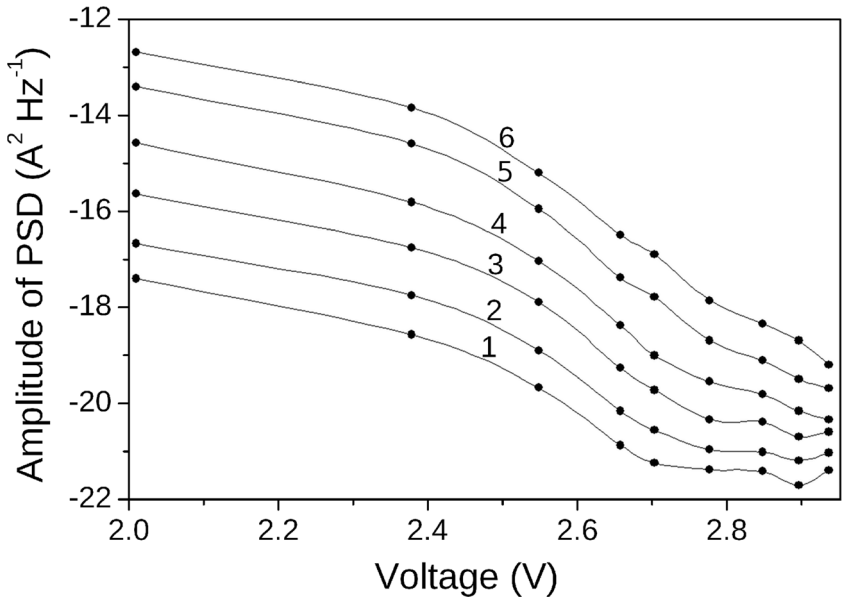


**Fig. 7** Dependencies of the decimal logarithm of PSD of the current noise on the constant voltage of discharge curve for different frequencies, Hz: 1—8.24, 2—3.03, 3—1.03, 4—0.40, 5—0.10, 6—0.04

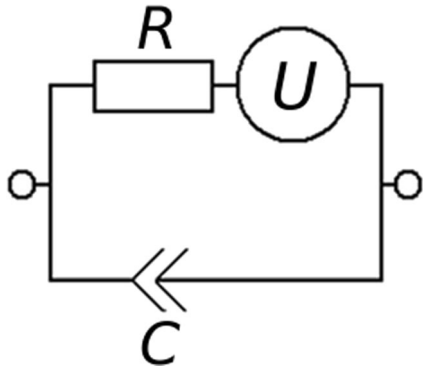


**Fig. 8** Model equivalent scheme with a frequency-independent source of voltage noise

the active part of the impedance and, therefore, is not a thermal noise (Nyquist noise). This conclusion is also confirmed by the fact that in terms of amplitude, the measured noise is several orders of magnitude higher than the thermal noise; this is easily verified by formula (1).

It can be concluded that in the case of the electrochemical system under consideration it is impossible to precisely describe the evolution of slopes of PSD frequency dependences by single high- or low-frequency CPE-R-circuit in the impedance data. This is due to the fact that none of the slopes calculated from impedance data, reaches the maximum slope value that is − 2.06. That means that the PSD slope of such high value can only be described by those joint actions when they are connected as a cascade and the second CPE-R pair additionally increases the slope created by a first pair. The additional reason for it is that even theoretical capacitor only has a RC circuit slope of − 2. But electrochemical systems double layer and another non-theoretical capacitances poses a lower exponent absolute values in their frequency dependence and they cannot reach the value of − 2.06 that is observed on PSD slope for lowest measured voltage. But if we connect two RC circuits in cascade the maximum theoretical SPD slope in this case will be equal to − 4.

It seems reasonable that the second RC circuit consists of the impedance elements of the low-frequency semicircle, since for it, there is an active increase in the exponent of the constant phase element just below the battery discharge voltage of 2.6–2.8 V, while at higher voltages this semicircle is weakly pronounced. This thesis agrees with the conclusions of the analysis of Figs. 5, 6, and 7 on the qualitative change of noise behavior during transition to the stages of battery-deep discharge.

As it can be seen, the simple model shown in Fig.8 cannot precisely describe the PSDs frequency dependences for the whole discharge curve of the battery under investigation. The model proposed in work [49] probably will face the same problem as it does not include cascaded elements which can form the PSD spectrum slope higher than − 2 by absolute value. The comparison of electrochemical impedance data and electrochemical noise method results shows that a more complicated model is required. It should be noted that such cascaded parallel types of equivalent circuits suitable for electrochemical noise modeling are used in electrochemical impedance investigations of Li-based batteries [47, 48]. Such modeling is a very interesting task as it can explain the noise PSDs behavior, and also it potentially can give some new information about the processes which generate electrochemical noise in electrochemical power sources, as there are works focused on finding those nature [51]. We hope to develop such model in our future works by deeper investigation of discussed battery type and by including other types of primary and secondary batteries in our investigations.

## Conclusions

For the first time, electrochemical noise of a $LiMnO_4$ lithium battery during its discharge on a constant resistance load was measured. The power spectral density of the noise is calculated for various stages of the discharge.

It was found that during the battery discharge process, the noise amplitude is shown to increase, as can be seen from the increase in the standard deviation of the discharge voltage, as well as from the increase in the values of the noise power spectral density spectrums. The dependence of the growth of the amplitude of power spectral densities of the current noise on the discharge voltage is nearly linear for frequencies below 1 Hz.

It was shown that for the studied types of batteries, the slope of the spectral power density changes from values close to − 1 to the ones close to − 2 and a little bit exceeds it as the discharge proceeds. In this case, the most pronounced changes occur in the range of discharge potentials of 2.9–2.6 V. Probably, the magnitude and slope of the frequency dependence of the spectral power density of noise can be considered as a discharge criterion for this battery type. The dependences obtained for electrochemical noise indicate that at the deep discharge, below voltages of 2.6 V, the frequency dependence of electrochemical noise changes for investigated battery type.

The electrochemical impedance spectrums were measured at different stages of the discharge process. For the first time, the attempt was made to compare the data obtained from the equivalent circuit analysis with the results of electrochemical noise investigation of $Li/MnO_2$primary lithium battery. It was found that some correlations exist between this two methods but traditional single-RC circuit model based on Faradic resistance and double-layer capacitance cannot precisely explain the behavior of electrochemical noise of the battery under study for the whole discharge curve of it. It is possible to conclude that more complex parallel type of modeling circuit is required. This work was supported by the State Task of Russian Federation (the state registration number 01201361853).

## References


1. Hu X, Li SE, Yang Y (2016) Advanced machine learning approach for lithium-ion battery state estimation in electric vehicles. IEEE Trans Trans Electrification 2(2):140–149
2. Bloom I, Walker LK, Basco JK, Malkow T, Saturnio A, de Marco G, Tsotridis G (2013) A comparison of fuel cell testing protocols – a case study: protocols used by the U.S. Department of Energy, European Union, International Electrotechnical Commission/Fuel Cell Testing and Standardization Network, and Fuel Cell Technical Team. J Power Sources 243:451–457
3. de Beer C, Barendse PS, Pillay P (2015) Fuel cell condition monitoring using optimized broadband impedance spectroscopy. IEEE Trans Ind Electron 62(8):5306–5316
4. Katayama N, Kogoshi S (2015) Real-time electrochemical impedance diagnosis for fuel cells using a DC–DC converter. IEEE Trans Energy Convers 30(2):707–713
5. Farmann A, Waag W, Sauer DU (2015) Adaptive approach for on-board impedance parameters and voltage estimation of lithium-ion batteries in electric vehicles. J Power Sources 299:176–188
6. Bertocci U, Huet F, Nogueira RP, Rousseau P (2002) Drift removal procedures in the analysis of electrochemical noise. Corrosion 58(4):337–347
7. Gabrielli C, Huet F, Keddam M (1986) Investigation of electrochemical processes by an electrochemical noise analysis. Theoretical and experimental aspects in potentiostatic regime. Electrochim Acta 31(8):1025–1039
8. Bertocci U, Huet F (1995) Noise analysis applied to electrochemical systems. Corrosion 51(2):131–144
9. Tyagai VA, Luk'yanchikova NB (1967) Equilibrium fluctuations in electrochemical processes. Elektrokhimiya (in Russian) 3:316–322
10. Tyagai VA (1971) Faradaic noise of complex electrochemical reactions. Electrochim Acta 16(10):1647–1654
11. Tyagai VA (1974) Noise in electrochemical systems. Elektrokhimiya 10:3–24
12. Barker GC (1969) Noise connected with electrode processes. J Electroanal Chem 21(1):127–136
13. Barker GC (1975) Large signal aperiodic equivalent electrical circuits for diffusion and faradaic impedances. J Electroanal Chem 58(1):5–18
14. Barker GC (1977) Faradaic reaction noise. J Electroanal Chem 82(1-2):145–155
15. Grafov BM (1966) On the equilibrium fluctuations in a stationary state. Elektrokhimiya 2:1249–1254
16. Grafov BM, Levich VG (1968) On the fluctuation-dissipation theorem in a stationary state. Sov Phys JETP 54:507–510
17. Martemyanov SA, Petrovskiy NV, Grafov BM (1991) Turbulent pulsations of the microelectrode limiting diffusion current. J Appl Electrochem 21(12):1099–1102
18. Grafov BM, Dobrovol'skii YA, Davydov AD, Ukshe AE, Klyuev AL, Astaf'ev EA (2015) Electrochemical noise diagnostics: analysis of algorithm of orthogonal expansions. Russ J Electrochem 51(6):503–507
19. Klyuev AL, Davydov AD, Grafov BM, Dobrovolskii YA, Ukshe AE, Astaf'ev EA (2016) Electrochemical noise spectroscopy: method of secondary Chebyshev spectrum. Russ J Electrochem 52(10):1001–1005
20. Grafov BM, Dobrovolskii YA, Klyuev AL, Ukshe AE, Davydov AD, Astaf'ev EA (2017) Median Chebyshev spectroscopy of electrochemical noise. J Solid State Electrochem 21(3):915–918
21. Singh PS, Lemay SG (2016) Stochastic processes in electrochemistry. Anal Chem 88(10):5017–5027
22. Martinet S, Durand R, Ozil P, Leblanc P, Blanchard P (1999) Application of electrochemical noise analysis to the study of batteries: state-of-charge determination and overcharge detection. J Power Sources 83(1-2):93–99
23. Legros B, Thivel PX, Bultel Y, Nogueira RP (2011) First results on PEMFC diagnosis by electrochemical noise. Electrochem Commun 13(12):1514–1516
24. Kanevskii LS (2009) Special features of discharge characteristics of different types of lithium–thionyl chloride cells and the problem of their diagnostics. Russ J Electrochem 45(8):835–846
25. Grafov BM, Kanevskii LS, Astafiev MG (2005) Noise characterization of surface processes of the Li/organic electrolyte interface. J Appl Electrochem 35(12):1271–1276
26. Astafev EA, Ukshe AE, Manzhos RA, Dobrovolsky Yu A, Lakeev SG, Timashev SF (2017) Flicker noise, spectroscopy, in,the analysis of electrochemical noise, of,hydrogen-air PEM, fuel,cell during its degradation. Int,J Electrochem Sci 12:1742–1754
27. Linden D, Reddy TB (eds) (2002) Handbook of batteries, 3rd edn. New York, McGrow-Hill
28. Aurbach D, Markovsky B, Levi MD, Levi E, Schechter A, Moshkovich M, Cohen Y (1999) New insights into the interactions between electrode materials and electrolyte solutions for advanced nonaqueous batteries. J Power Sources 81–82:95–111
29. Dose WM, Sharma N, Donne SW (2014) Discharge mechanism of the heat treated electrolytic manganese dioxide cathode in a primary Li/$MnO_2$ battery: an in-situ and ex-situ synchrotron X-ray diffraction study. J Power Sources 258:155–163
30. Ohzuku T, Kitagawa M, Hirai T (1989) Electrochemistry of manganese dioxide in lithium nonaqueous cell. I X-ray diffractional study on the reduction of electrolytic manganese dioxide. J Electrochem Soc 136:3169–3174
31. Padhi AK, Nanjundaswamy KS, Goodenough JB (1997) Phospho-olivines as positive-electrode materials for rechargeable lithium batteries. J Electrochem Soc 144(4):1188–1194
32. Srinivasan V, Newman J (2004) Discharge model for the lithium iron-phosphate electrode. J Electrochem Soc 151(10):A1517–A1529
33. Van der Ven A, Bhattacharya J, Belak AA (2013) Understanding Li diffusion in Li-intercalation compounds. Acc Chem Res 46(5):1216–1225
34. Tan H, Wang S (2014) Kinetic behavior of manganese dioxide in Li/$MnO_2$ primary batteries investigated using electrochemical impedance spectroscopy under nonequilibrium state. 161:A1927–A1932
35. Liu Q, Wang S, Cheng H (2013) High rate capabilities Fe-doped EMD electrodes for li/$MnO_2$ primary battery. Int J Electrochem Sci 8:10540–10548
36. Wang S, Liu Q, Yu J, Zeng J (2012) Anisotropic expansion and high rate discharge performance of V-doped $MnO_2$ for Li/$MnO_2$ primary battery. Int J Electrochem Sci 7:1242–1250
37. Astafev EA (2018) Multi-purpose high resolution device for measurement of electrochemical noise. Prib Tekh Eksp1:151–152
38. Nyquist H (1928) Thermal agitation of electric charge in conductors. Phys Rev 32(1):110–113
39. Martemianov S, Adiutantov N, Evdokimov YK, Madier L, Maillard F, Thomas A (2015) New methodology of electrochemical noise analysis and applications for commercial Li-ion batteries. J Solid State Electrochem 19(9):2803–2810
40. Bartlett MS (1948) Smoothing periodograms from time-series with continuous spectra. Nature 161(4096):686–687
41. Welch PD (1967) The use of fast Fourier transform for the estimation of power spectra: a method based on time averaging over short, modified periodograms. IEEE Trans Audio Electroacoust 15(2):70–73
42. Astafev EA, Ukshe AE, Gerasimova EV, Dobrovolsky YA, Manzhos RA (2018) Electrochemical noise of a hydrogen-air polymer electrolyte fuel cell operating at different loads. J Solid State Electrochem 22(6):1839–1849

43. Astafev EA, Ukshe AE, Dobrovolsky Yu A (2018) The model of electrochemical noise of a hydrogen-air fuel cell. J Electrochem Soc 165(9):F604–F612. https://doi.org/10.1149/2.0251809jes
44. Astaf'ev EA (2018) Electrochemical noise measurement of polymer membrane fuel cell under load. Russ J Electrochem 54(6):554–560
45. Timashev SF (2007) Flicker-noise spectroscopy: information in chaotic signals. Fizmatlit, Moscow
46. Timashev SF, Polyakov YS (2007) Review of flicker noise spectroscopy in electrochemistry. Fluct Noise Lett 7(02):R15–R17
47. Li SE, Wang B, Peng H, Hu X (2014) An electrochemistry-based impedance model for lithium-ion batteries. J Power Sources 258:9–18
48. Jean-Marcel A, Joze M, Stane P, Miran G (2010) On the interpretation of measured impedance spectra of insertion cathodes for lithium-ion batteries. J Electrochem Soc 157(11):A1218–A1228
49. Hassibi A, Navid R, Dutton RW, Lee TH (2004) Comprehensive study of noise processes in electrode electrolyte interfaces. J Appl Phys 96(2):1074–1082
50. Beletskiy AF (1967) An introduction to the principles of linear circuits. Svyaz, Moscow
51. Kuparowitz T, Sedlakova V, Sedlak P, Sikula J (2017) Low frequency noise of electrochemical power sources. In Noise and Fluctuations (ICNF), 2017 International Conference on. IEEE 1-4